

EARTHQUAKE PREDICTION, IONOSPHERIC TOTAL ELECTRON CONTENT, AND THREE EARTHQUAKES IN CALIFORNIA

by

Ahmet Yuçel URUSAN

Department of Civil Engineering, Faculty of Engineering and Architecture,
Istanbul Gelisim University, Avcilar, Istanbul, Turkey

Original scientific paper
<https://doi.org/10.2298/TSCI181106340U>

Because it is a newer and unproven technique, ionospheric seismology is still accepted as a phenomenon by a lot of scientists. However, research in this subject is rapidly increasing in the last decade. According to the ionospheric seismology, the mechanical energy accumulated by the compression of the rocks before the big earthquakes is released from the ground by creating a positive hall. These processes at the ground-to-air interface can lead to the injection of massive amounts of air ions into the lower atmosphere [1]. As a result of the injection, the earthquake lights, temperature rising, the pressure in the troposphere, radio frequencies distortions, and total electron content perturbation in ionosphere occur. Therefore, even if it does not enough alone, this parameter can be contributing to earthquake predict. It has been supported with several instances of manuscript. In this study, ionospheric total electron content was calculated for each station and satellite using GPS stations data in California, USA, for three last earthquakes. The earthquakes are named Hector Mine-1999, Baja-2009, and Napa-2014, and their magnitudes are 7.1, 7.2, and 6, respectively. After the processes, quite significant outcomes have been obtained.

Key words: earthquake, earthquake prediction, GNSS, GPS, ionosphere, total electron content, piezoelectric

Introduction

Normally, ionosphere includes ion and electron that depend on day and night time, seasons and latitudes. Because geomagnetic storm, which generated by a solar wind storm or/and heliospheric disturbances of a solar magnetic field, which interacts with the Earth's magnetic field, creates large disturbances in the ionosphere and they also change in the time of solar storm period. The geomagnetic storms enhance the ionosphere and increase the total number of ionospheric electrons, fig. 1. Therefore, the GPS signals from satellites, 20200 km above, to fixed stations on Earth, need some correction models and this dynamic boost and errors are introduced into the position calculations [2]. Additionally, electron launching, and earth's magnetic irregularities are produced by earthquakes which compose defects of total electron content (TEC). This event occurs both pre-seismic and co-seismic time [3, 4]. All models about atmosphere are generated with routine and long period data for using in GPS data processing. On the contrary, these suddenly events are not modeled. These short time changes can only be measured by regularly in the troposphere as temperature, pressure, humidity and calculated as TEC

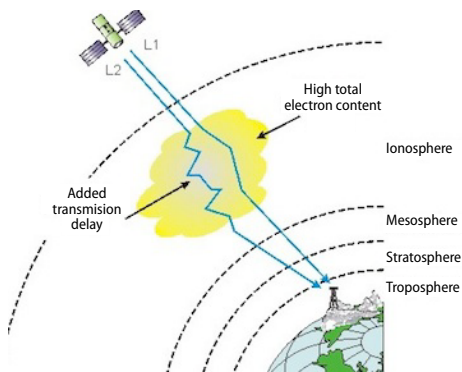


Figure 1. The L1 and L2 signals broadcast from GPS satellite to reference station

for ionosphere. An investigation by Zhang *et al.* [5] also shows that the outgoing longwave radiation anomaly occur before some earthquakes which triggered by tidal-force [5]. The 2011 Thoko-Oki (M_w 9.0), 2010 Chile (M_w 8.8), 2004 Sumatra-Andaman (M_w 9.2), and 1994 Hokkaido-Toho-Oki (M_w 8.3) earthquakes are greater than 8.0 M_w . All of these are perceived before they happen almost sixty minutes by the TEC prominent irregularities which bound up with magnitude [6, 7]. As some significant conclusions about earthquake prediction using ionospheric TEC anomalies was also obtained on GPS signals for Van earthquake occurred eastern part of Turkey, tab. 1. There was seen that

the pre-sign of the earthquake was started on GPS signals 51 minutes before the event [8].

Continuously operating reference stations system supplies an chance for radio frequency wave spread monitor and we can comb out whether TEC values are small or large related daily ionospheric change [9]. The TEC has a maximum value at noon due to the Sun is directly overhead, and it has a minimum value at night because of the lack of Sun. Because the solar activities are followed all time to save communication and satellite(s) activities in the world and its' around, they are observed, before they reached to the earth's atmosphere. But it is difficult to follow strain accumulating based underground energy in the atmosphere. Any prediction could not be done about when and from where the energy would be discharged from the

Table 1. Earthquake features list

Earthquake	Date	Time [PDT]	Magnitude [M_w]	Depth [km]	Areas	Latitude	Longitude	GPS day
Hector Mine	Oct 16, 1999	2:46:44 am	7.1	0.1	Cal.	34.600° N	116.267° W	289
Baja	Apr 4, 2010	3:40:41 pm	7.2	10	Mexico	32.128° N	115.303° W	94
Napa	Aug 24, 2014	3:20:44 pm	6.0	11.3	North Bay – Cal.	38.220° N	122.313° W	236
Van	Oct 23, 2011	1:41:20 pm	7.1	15	Eastern Turkey	38.689° N	43.465° W	296



Figure 2. Alum Rock earthquake and the magnetometers; one of them is far away around 2 km from the epicenter

ground to the atmosphere. It could be measured stress accumulation before discharged as an electric field or unipolar magnetic pulses and combined with TEC perturbation after discharged.

Pre-earthquake electromagnetic waves typically have frequencies between 0.01Hz and 20Hz, because just low-frequency ingredient may traverse tens of kilometers through rock column. They have been independently observed prior many

earthquakes over the past 50 years [10-12]. Within the weeks leading up to the $M_w = 5.4$ Alum Rock earthquake of Oct. 30, 2007, a magnetometer far away around 2 km from the epicenter, recorded abnormal un-alternating magnetic pulses, reaching amplitudes up to 30 nTesla [13], fig. 2. The ratio of these strokes increased as the event day approached. A double of magnetometer stations in Peru recently recorded similar unipolar strokes prior to several medium-sized earthquakes and triangulating the source of these pulses caught out the location of next earthquake epicenters [10-12].

The K_p index

The official planetary K_p index is derived by calculating a weighted average of K indices from a network of geomagnetic observatories [14]. The K index was introduced by Julius Bartels in 1939 [15]. Since the observatories do not report their data in real-time, various operations centers around the globe estimate the index based on data available from their local network of observatories [16]. The K_p is an excellent indicator of disturbances in the Earth's magnetic field, and it is used by National Oceanic and Atmospheric Administration (NOAA) – Space Weather Prediction Center to decide whether geomagnetic alerts and warnings need to be issued for users who are affected by these disturbances.

The GPS data for each station

The GPS satellites have two revolutions in a day in their orbits. These two periods could be calculated and seen as a sample TEC volume in fig. 3. Here, the second duration is longer than the first one. Because the observation time is depending on the satellite's elevation angle, it is a maximum of 6 hours for a station per period. This means that it can be observed by a station in this time. However, it required to pass over its values which are under the elevation angle 10° for a good approach. In the initial time, the TEC changing ratio usually is bigger than the middle of the observation time, if there is not any anomaly. In the graphs, since the satellites are close to the horizon line, the TEC values grow in the beginning and end of the transitional period of the satellites.

On the other hand, the probability of obtaining meaningful result depends on station and epicenter distance, earthquake magnitude, depth of earthquake and position of the satellites.

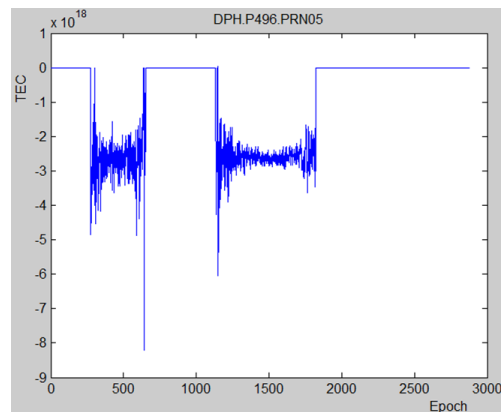


Figure 3. Sample for daily TEC changing chart for two of period

Applications and discussions

In this study, TEC variability was investigated before last three earthquakes equal or greater than $6 M_w$ in California using GPS data. These earthquakes are Napa, Baja and Hector Mine, tab. 1.

Hector Mine

This earthquake was investigated by some scientist such as Afraimovich *et al.* [17], Thomas *et al.* [18], Pulinet *et al.* [19], Su *et al.* [20]. They usually sign out different results

to each other. While Pulnits *et al.* [19] identified unnatural changes in TEC commencing one week prior to the mainshock, Afraimovich *et al.* [17] finalized that TEC changes close to the epicenter were controlled by solar and geomagnetic activity that were disinterested in earthquake. On the other hand, Thomas *et al.* [18] claimed that the signal anomalies occurred because of apparatus defect or global, solar-driven changeability. All of them have used the same 13 GPS reference stations. However, Afraimovich, Su and their groups have also used two reference regions in Europe and Japan besides these stations, having a similar magnetic latitude of the Hector Mine region, to comparing TEC data. Thomas *et al.* [18] processed more two stations that are in Canada very far from the epicenter.

The 13 GPS stations have been used in this research, and they are shown in tab. 2, fig. 4. The stations are within the radius of 1200 km of the epicenter. However, a different data evaluation method is used to analysis TEC anomalous in this study. Unlike the others, TEC anomalous were been examined for each station and satellite using 30 sec-GPS data, recorded for 1 month. In the region below 10° on the horizon and short-term TEC values were not considered.

Table 2. Reference stations are within 1200 km of the eq epicenter

Station number	Station name	Geodetic latitude [°]	Geodetic longitude [°]	Magnetic latitude [°]	Distance from epicenter [km]
1	GOL2	35.42	-116.88	41.91	107
2	SIO3	32.86	-117.25	39.20	214
3	CAT1	33.44	-118.48	39.55	241
4	SCIP	32.91	-118.48	39.00	278
5	FERN	35.34	-112.45	42.74	357
6	HARV	34.46	-120.68	40.14	405
7	ECHO	37.91	-114.26	45.01	410
8	CASA	37.64	-118.89	43.77	412
9	COSA	33.56	-111.88	41.02	420
10	FRED	36.98	-112.49	44.42	431
11	FARB	37.69	-123.00	42.95	695
12	PIE1	34.30	-118.11	42.53	748
13	AZCN	36.83	-107.91	45.17	794

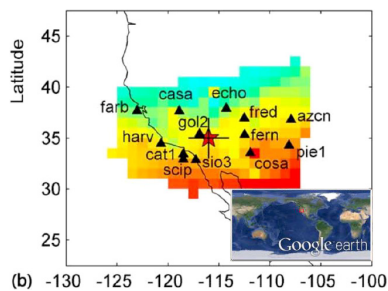


Figure 4. Earthquake epicenter and GPS reference stations

is around midnight, and the K_p value should be at a low level for this region at the time. For this reason, it may be said that the TEC disturbance, was seen in the chart, is significant about earthquake prediction. Another two disturbances are seen at 6 o'clock on October 19 and Oc-

First of all, there are patterns, approximately same each other, were seen in daily TEC charts for each satellite signal according to the stations. But, due to electromagnetic pulse, generated by rock stress, coming from Earth Crust, the patterns are changing in an unexpected time in same epoch of some days for different stations and satellites. The TEC scintillation was obtained for seven satellites in epoch 90, and it is shown in fig. 7. This means an electromagnetic pulse was generated and emitted by the ground at 00:45 a. m., four days before the event, in October 12th. It may be thought that the reason of this disturbance is high K_p values. But the hour

tober 20, the K_p index is very low in these days. When the seismic data is considered, it shows some small foreshocks, maximum $3.8 M_w$, are occurred 20 hours before the main shock, according to California Institute of Technology seismic data [22]. Otherwise, the magnitude of completeness, M_c , with time for the Hector Mine aftershock sequence can be seen in fig. 6. There, stars plotted along the base represent all aftershocks $M_c \geq 5.0$. If two figures are correlated, these can be said:

- First pulse in October 12 is pre-earthquake signal, (figs. 5 and 7),
- The pulses in October 19 and October 20 (4-6 days with stars) after the earthquake in fig. 6 were generated by the aftershocks in fig. 5.

There is a sample about templates in TEC charts in fig. 8. It belongs COSA station – PRN30 satellite between 276 and 296 GPS days. Although, there are some anomalies are seen on October 12th (GPS day 285) before the earthquake and October 19th, October 20th (GPS days 292 and 293) after the earthquake for CASA station in both figs. 5 and 7, TEC values have only one pattern for 20 days like in fig. 8 for COSA station. And, other station concerned have their own pattern like COSA except CASA. Therefore, it can be said that the solutions, which have been shown in figs. 5 and 6 and explained in the related paragraph above, are very significant for CASA station. Finally, it can be said that the TEC disturbance in fig. 7 is a pre-earthquake sign.

Baja

Baja is in the Southern California near the Mexico border. There are 8 GPS, fig. 9 reference stations in around Baja were used in the process. The GPS stations are P066, P494, P496, P500, P003, P001, IID2, and GMPK. All of them are surrounding from north of the epicenter. The closest GPS stations to the epicenter are P500, P496, and P494 as ascending, and the distances are 29.7 miles, 37.61 miles, and 43.82 miles, respectively.

At this point, fig. 10 gives very important tips about relationships of between satellite, stations, epicenter, and TEC changing chart for

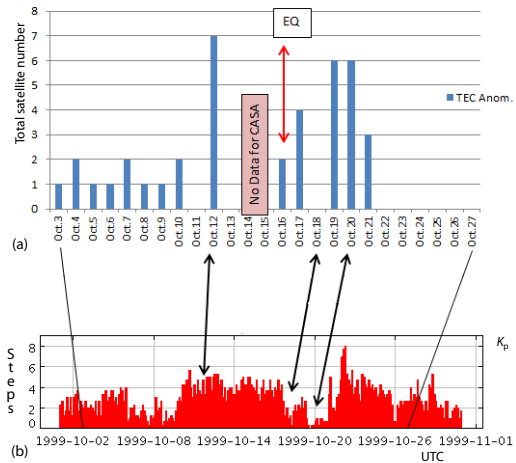


Figure 5. (a) Hector Mine earthquake cumulative TEC anomalies, (b) K_p index

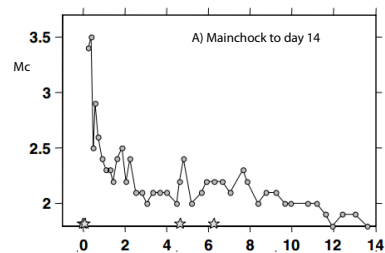


Figure 6. The magnitude of completeness (M_c) with time for the Hector Mine aftershock sequence [21]

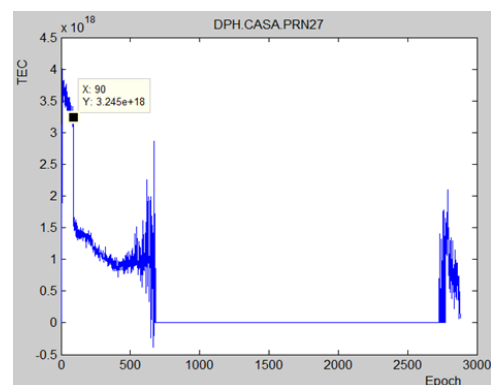


Figure 7. The TEC variability for GPS day 285 (October 12, 1999) were obtained using CASA station data; there could be seen seven satellites' daily TEC anomalies; the satellites are named as PRN01, PRN03, PRN13, PRN18, PRN19, PRN27, PRN37

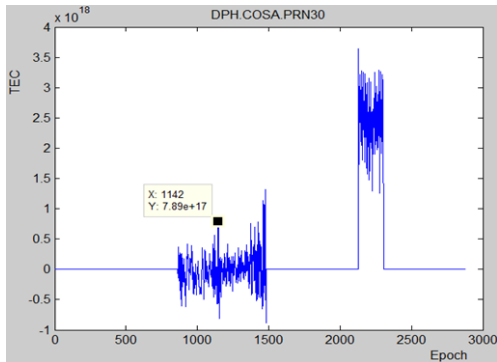


Figure 8. The TEC values for COSA station PRN30 satellite between 276-296



Figure 9. Baja earthquake epicenter and reference stations

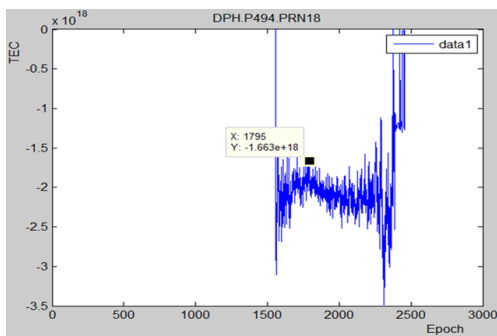


Figure 10. The TEC deformations are observed in three GPS reference stations for PRN18 satellite in the event day (94); as a significant result is that the epoch number, initial of the deformations, is depend on directly proportional to the distance between earthquake epicenter and station

event day. In such a way that fig. 10 shows that TEC changing was observed by P500, P496, and P494 stations. The event epoch is 1882, and all perturbation epochs are 1768, 1787, and 1795 for P500, P496, and P494 stations, respectively. All distortions occurred before the event, and they are, according to their occurred time, depend on directly proportional to the distance between earthquake epicenter and station. That means, the closest station is P500, and the TEC deformation has been seen in that station's data as the first. Additionally, because of the comparing charts to each other about TEC changing ratio with noise and length of the observation periods, It can be also said that the satellite is almost over of the epicenter. The graphs which are shown in fig. 10 really shows a deformation. On the other hand, the K_p index is at low level before and in the event day, fig. 12. This case shows the reason of deformation is not Solar storms. Although, they are concluded that they are a pattern for this satellite and stations in this period, they have great noisy, if 93 and earlier 10 days examined (the event day is 94). Unfortunately, because there is no any GPS station in southern of Baja, the process could not run for the region.

Another different anomaly was observed by P496 reference station, fig. 11. There is a negative pulse in epoch 1816 and 33 minutes before the major earthquake in the event day. The reason of this pulse can be a rocket engine or supersonic engine. On the other hand, because this pulse was obtained when the satellite is close or below the horizon line, it has not been considered as TEC deformation. It was also not sensed by other stations or a different satellite signal data at the same station. It is important to separate the anomalies to each other for defining anomaly pattern sets.

Napa

To analyze pre-earthquake signals in ionospheric TEC disturbances, 11 GPS reference stations were used in the process. Their names are P202, P264, VCVL, P198, P199, P200, P261, P262, P181, P224, P194, fig. 13.

The most remarkable solutions were obtained from P200, P261, and P264 stations, and their distances to the epicenter are respectively 7.48 miles, 6.74 miles, and 16.64 miles. One of them, named P261, is more significant than the others. The TEC charts were controlled carefully for each satellite at this step. The TEC distortion is seen for the PRN05 satellite at this station in fig. 14. There are two periods, signed (a) and (b), can be seen in fig. 14. In such a way that, in the event day, the first period, which has shown in fig.14(a), has not been expected pattern for last three days before the earthquake. The second pass of the satellite PRN05 gives the chart in part fig.14(b) of the figure, and this pattern is almost same to each other for before two and earlier days, so the anomaly can be thought as normal. In addition to this, the K_p values highly raised, to five, on August 12th and August 19th, and it was very silent between August 20th and August 27th before and after the earthquake day, have been shown in fig. 15. Therefore, the anomalies in TEC in the last three days before the earthquake have been a result of the earthquake stress in rocks, fig. 14.

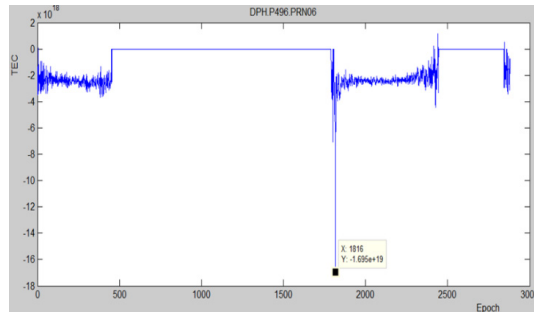


Figure 11. Negative pulse was sensed by P496 station

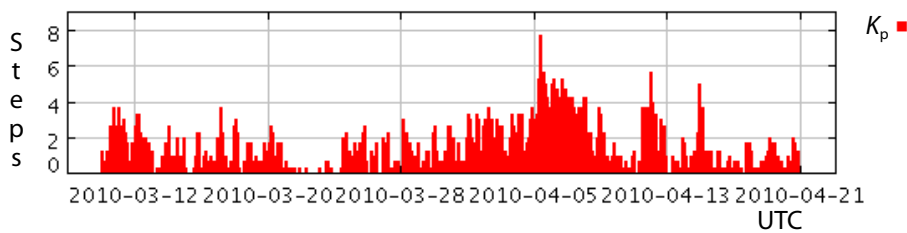


Figure 12. The K_p index chart before and after Baja earthquake

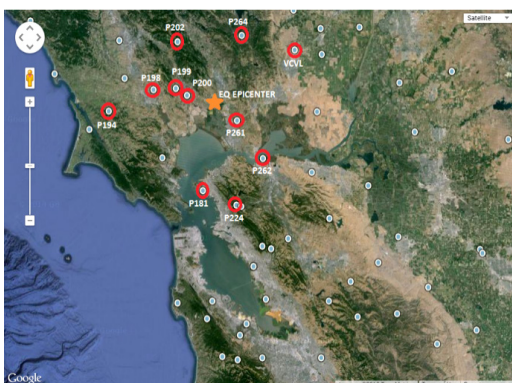


Figure 13. Napa earthquake and selected 11 stations to calculate TEC changing before and after the earthquake time; the most remarkable solutions were obtained from three of them

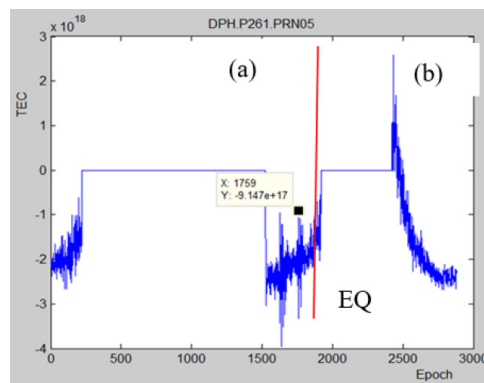


Figure 14. Daily TEC changing chart; there is seen absolute distortion in epoch 1732 before Napa earthquake (1842)

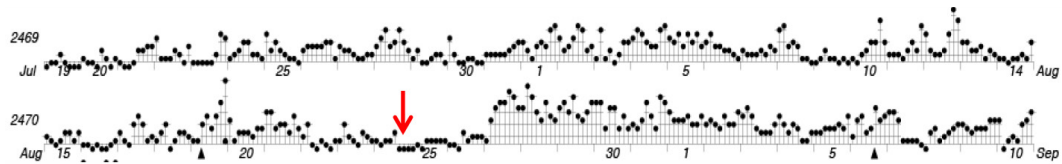


Figure 15. The K_p changing chart before and after Napa earthquake

Conclusions

In this investigation, three big earthquakes in California, equal to and greater than $6.0 M_w$, have been reviewed about their relationships with ionospheric TEC. The events are 1999-Hector Mine, 2010-Baja, and 2014-Napa earthquakes.

The most significant solution has been obtained for the Hector Mine earthquake. From the 13 GPS stations analyzed, only a significant result was obtained from the CASA station data. The CASA station has some TEC anomalies for the PRN18 satellite in 285, 291, and 292 GPS days before and after the earthquake due to the electromagnetic field, generated by rock stress. Especially, TEC scintillation was obtained for seven satellites in epoch 90. That means an electromagnetic pulse was generated and emitted by the ground at 00:45 a. m., four days before the event, in October 12th. Since the hour is around midnight, and the K_p value should be in low level for this region at the time, the reason of the scintillation is not the high K_p values. Thus, it may be said that the TEC disturbance is significant about earthquake prediction. Another two disturbances are seen at 6 o'clock on October 19 and October 20, the K_p index is very low in these days. When the seismic data is considered, it was seen that two aftershocks, bigger than $5 M_w$, occurred after the main shock. Their date is compatible with the charts. The other stations have its own patterns but no TEC anomalies in there.

Since there are not GPS reference stations in the southern region of the Baja earthquake epicenter in the event time, there only the stations in the northern of Baja could be examined. Therefore, 8 GPS, fig. 11, reference stations in around Baja were used in the process. According to available stations data, TEC changing was only observed by P500, P496, and P494 stations. The event epoch is 1882, and all perturbation epochs are 1768, 1787, and 1795 for P500, P496, and P494 stations, respectively. All distortions occurred before the event, and they are, according to their occurred time, depend on directly proportional to the distance between earthquake epicenter and station. That means, the closest station is P500, and the TEC deformation has been seen in that station's data as the first. Additionally, there is a negative pulse in epoch 1816, and 33 minutes before the major earthquake. The reason of this pulse can be a rocket engine or supersonic engine. On the other hand, because this pulse was obtained when the satellite is close or below the horizon line, it has not been considered as TEC deformation.

For NAPA earthquake, the most remarkable solutions were obtained from 3 of 11 GPS stations, which are named P200, P261, and P264. Their distances to the epicenter are respectively 7.48 miles, 6.74 miles, and 16.64 miles. The TEC distortion for P261 station was especially seen for PRN05 satellite. The distortion, shown by a black circle in fig. 14, for first passing period per day in the last three days, including the event day as last day, has not been expected pattern. The second pass per day of the satellite PRN35 gives the chart in part 14(b) of the figure, and this pattern is almost same to each other for before two and earlier days, so that can be thought as normal.

There have quite meaningful results been obtained for three earthquakes. These and others are a big contribution to the earthquake prediction research. Despite, a lot of earthquakes

have been investigated and found highly significant solutions, there is not any full precise result about earthquake prediction due to TEC using GPS data. In this mean, the faults and rock stress must be trace continuously by magnetometers and obtained some interferometric solutions in both space and time [23]. These solutions must be combined with TEC solutions for more strong results to prediction earthquakes.

Acknowledgment

Author wishes to thank Shimon Wdowinski for inviting to use the facilities at the University of Miami - RSMAS and sharing his knowledge and experiences. He wishes to thank Ugur KAYNAK for also sharing his knowledge and experiences. He also wishes to thank NOAA for free GPS stations data. He wants to say thank to Google Technology Company for mapping interface. Finally, he wishes to thank MIT for GAMIT program.

References

- [1] Freund, F., Pilorz, S., Electric Currents in the Earth Crust and the Generation of Pre-Earthquake ULF Signals, in: *The Frontier of Earthquake Prediction Studies*, (Ed. Hagakawa, M.), Nihon Senmontosho Publ., Tokyo, 2012, pp. 468-508
- [2] ***, NOAA, Space Weather and GPS Systems, <http://www.swpc.noaa.gov/impacts/space-weather-and-gps-systems>
- [3] Calais, E., Minster, J. B., GPS Detection of Ionospheric Perturbations Following the January 1994, Northridge Earthquake, *Geophysics Res. Lett.*, 22 (1995), 9, pp. 1045-1048
- [4] Bajčetić, J. B., *et al.*, Ionospheric D-Region Temperatures Relaxation and Its Influences on Radio Signal Propagation After Solar X-Flares Occurrence, *Thermal Science*, 19 (2015), Suppl. 2, pp. S299-S309
- [5] Zhang, X., *et al.*, Study on Thermal Anomalies of Earthquake Process by Using Tidal-Force and Outgoing-Longwave-Radiation, *Thermal Science*, 22 (2018), 2, pp. 767-776
- [6] Heki, K., Ionospheric Electron Enhancement Preceding the 2011 Thoku-Oki Earthquake, *Geophysical Research Letters*, 38 (2011), 17, L17312
- [7] Pulinet, S., Davidenko, D., Ionospheric Precursors of Earthquakes and Global Electric Circuit, *Advances in Space Research*, 53 (2014), 5, pp. 709-723
- [8] Urusan, A., (2014), Relations between the GNSS, InSAR, and the other Techniques for Prediction of Earthquakes, *Arabian Journal of Geosciences*, 8 (2015), 9, pp. 7631-7642
- [9] Ducic, V., *et al.*, Ionospheric Remote Sensing of the Denali Earthquake Rayleigh Surface Wave, *Geophysical Research Letters*, 30 (2003), 18, 1951
- [10] Bleier, T., *et al.*, Investigation of ULF Magnetic Pulsations, Air Conductivity Changes, Infrared Signatures Associated with the 30 October 2007 Alum Rock M5.4 Earthquake, *Nat. Hazards Earth Syst. Sci.*, 9 (2009), 2, pp. 585-603
- [11] Fraser-Smith, A. C., Ultralow-Frequency Magnetic Fields Preceding Large Earthquakes, *Eos*, 89 (2008), 23, p. 211
- [12] Héraud, J., *et al.*, *Determining Future Epicenters by Triangulation of Magnetometer Pulses in Peru*, AGU Fall Meeting, Washington DC, 2013, section NH014
- [13] Bortnik, J., *et al.*, Estimating the Seismotelluric Current Required for Observable Electromagnetic Ground Signals, *Ann. Geophysics*, 28 (2010), 8, pp.1615-1624
- [14] Bartels, J., The Technique of Scaling Indices K and Q of Geomagnetic Activity, in: *Annals of the International Geophysical*, Pergamon Press, Oxford, UK, 1957, Vol. 4, pp. 215-226
- [15] Bartels, J., The Standardized Index Ks and the Planetary Index Kp, *IATME Bulletin*, 12b (1949), pp. 97-120
- [16] Bartels, J., *et al.*, The Three-Hour Range Index Measuring Geomagnetic Activity, *Journal of Geophysical Research*, 44 (1939), 4, pp. 411-454
- [17] Afraimovich, E. L., *et al.*, Variations of the Total Electron Content in the Ionosphere from GPS Data Recorded during the Hector Mine Earthquake of October 16, 1999, California, *Russ. J. Earth Sci.*, 6 (2004), 5, pp. 339-354
- [18] Thomas, J. N., *et al.*, On the Reported Ionospheric Precursor of the 1999 Hector Mine, California Earthquake, *Geophys. Res. Lett.*, 39 (2012), 6, L06302

- [19] Pulinet, S. A., *et al.*, Special Case of Ionospheric Day-to-Day Variability Associated with Earthquake Preparation, *Advances in Space Research*, 39 (2007), 5, pp. 970-977
- [20] Su, Y. C., *et al.*, (2013), Temporal and Spatial Precursors in Ionospheric Total Electron Content of the 16 October 1999 Mw 7.1 Hector Mine Earthquake, *Journal of Geophysical Research: Space Physics*, 118 (2013),10, pp. 6511-6517
- [21] Wiemer, S., *et al.*, Properties of the Aftershock Sequence of the 1999 Mw 7.1 Hector Mine Earthquake, *Implications for Aftershock Hazard Bulletin of the Seismological Society of America*, 92 (2002), 4, pp. 1227-1240
- [22] ***, CALTECH, Significant Earthquakes and Faults, <http://scedc.caltech.edu/significant/hectormine1999.html>
- [23] Scoville, J., *et al.*, Pre-Earthquake Magnetic Pulses, *Nat. Hazards Earth Syst. Sci. Discuss.*, 15 (2014), 8, pp. 7367-7381